J|A|C|S
ARTICLES
Published on Web 09/10/2004

Molecular Understanding of the Formation of Surface Zirconium Hydrides upon Thermal Treatment under Hydrogen of [(≡SiO)Zr(CH_2tBu)$_3$] by Using Advanced Solid-State NMR Techniques

Franck Rataboul,[†] Anne Baudouin,[†] Chloé Thieuleux,[†] Laurent Veyre,[†] Christophe Copéret,*[,†] Jean Thivolle-Cazat,[†] Jean-Marie Basset,*[,†] Anne Lesage,[‡] and Lyndon Emsley*[,‡]

Contribution from the Laboratoire de Chimie Organométallique de Surface (UMR 9986 CNRS/ESCPE Lyon), ESCPE Lyon, F-308-43 Boulevard du 11 Novembre 1918, F-69616 Villeurbanne Cedex, France, and Laboratoire de Chimie (UMR 5532 CNRS/ENS), Laboratoire de Recherche Conventionné du CEA (23V), Ecole Normale Supérieure de Lyon, 46 Allée d'Italie, F-69364 Lyon Cedex 07, France

Received September 12, 2003; E-mail: coperet@cpe.fr

Abstract: The reaction of [(≡SiO)Zr(CH_2tBu)$_3$] with H_2 at 150 °C leads to the hydrogenolysis of the zirconium−carbon bonds to form a very reactive hydride intermediate(s), which further reacts with the surrounding siloxane ligands present at the surface of this support to form mainly two different zirconium hydrides: [(≡SiO)$_3$Zr−H] (**1a**, 70−80%) and [(≡SiO)$_2$ZrH_2] (**1b**, 20−30%) along with silicon hydrides, [(≡SiO)$_3$SiH] and [(≡SiO)$_2$SiH_2]. Their structural identities were identified by ^{1}H DQ solid-state NMR spectroscopy as well as reactivity studies. These two species react with CO_2 and N_2O to give, respectively, the corresponding formate [(≡SiO)$_{4-x}$Zr(O−C(=O)H)$_x$] (**2**) and hydroxide complexes [(≡SiO)$_{4-x}$Zr(OH)$_x$] (x = 1 or 2 for **3a** and **3b**, respectively) as major surface complexes.

Introduction

Surface organometallic chemistry has been directed at designing and preparing single-site heterogeneous catalysts.[1] One of the key aspects of this field is to ascertain the structural identity of the so-called surface complex, which allows, in fine, structure−activity correlations, and thereby a rational improvement of the targeted catalysts. Therefore, it is necessary to rely on several chemical and spectroscopic methods, and one of the goals of surface organometallic chemistry is to develop new or improved tools for the characterization of surface complexes. We have recently implemented solid-state two-dimensional (2D) heteronuclear NMR correlation (HETCOR) techniques to probe surface structures at a molecular level, which has helped us to solve the structure of surface well-defined perhydrocarbyl complexes monografted on the surface of silica.[2−5] By well-defined species, we mean a metal for which the first coordination sphere is defined; that is, the number of covalent (or ionic) bonds with the surface and the number and types of other ligands are known. We and others have also been able to generate and characterize bisgrafted species upon controlling the thermal treatment of silica prior to its reaction with the molecular organometallic complex.[6−8]

The surface complex [(≡SiO)Zr(CH_2tBu)$_3$], a well-defined species, upon a thermal treatment under H_2 was reported to be transformed selectively into a trisgrafted species, [(≡SiO)$_3$Zr−H] (**1a**), according to IR and EXAFS spectroscopies.[9−17] Notably, this system displays high reactivity toward alkanes: (1) low-temperature activation of alkanes,[18] (2) fast H/D

[†] Laboratoire de Chimie Organométallique de Surface, ESCPE Lyon.
[‡] Laboratoire de Chimie, ENS Lyon.

(1) Copéret, C.; Chabanas, M.; Petroff Saint-Arroman, R.; Basset, J.-M. *Angew. Chem., Int. Ed.* **2003**, *42*, 156.
(2) Petroff Saint-Arroman, R.; Chabanas, M.; Baudouin, A.; Copéret, C.; Basset, J.-M.; Lesage, A.; Emsley, L. *J. Am. Chem. Soc.* **2001**, *123*, 3820.
(3) Chabanas, M.; Quadrelli, E. A.; Fenet, B.; Copéret, C.; Thivolle-Cazat, J.; Basset, J.-M.; Lesage, A.; Emsley, L. *Angew. Chem., Int. Ed.* **2001**, *40*, 4493.
(4) Lesage, A.; Emsley, L.; Chabanas, M.; Copéret, C.; Basset, J.-M. *Angew. Chem., Int. Ed.* **2002**, *41*, 4535.
(5) Chabanas, M.; Baudouin, A.; Copéret, C.; Basset, J.-M.; Lukens, W.; Lesage, A.; Hediger, S.; Emsley, L. *J. Am. Chem. Soc.* **2003**, *125*, 492.
(6) Amor Nait Ajjou, J.; Scott, S. L. *Organometallics* **1997**, *16*, 86.
(7) Amor Nait Ajjou, J.; Rice, G. L.; Scott, S. L. *J. Am. Chem. Soc.* **1998**, *120*, 13436.
(8) Lefort, L.; Chabanas, M.; Maury, O.; Meunier, D.; Copéret, C.; Thivolle-Cazat, J.; Basset, J.-M. *J. Organomet. Chem.* **2000**, *593*−*594*, 96.
(9) Zakharov, V. A.; Dudchenko, V. K.; Paukstis, E.; Karakchiev, L. G.; Ermakov, Y. I. *J. Mol. Catal.* **1977**, *2*, 421.
(10) Schwartz, J.; Ward, M. D. *J. Mol. Catal.* **1980**, *8*, 465.
(11) Yermakov, Y. I.; Ryndin, Y. A.; Alekseev, O. S.; Kochubei, D. I.; Shmachkov, V. A.; Gergert, N. I. *J. Mol. Catal.* **1989**, *49*, 121.
(12) Zakharov, V. A.; Ryndin, Y. A. *J. Mol. Catal.* **1989**, *56*, 183.
(13) Quignard, F.; Choplin, A.; Basset, J. M. *J. Chem. Soc., Chem. Commun.* **1991**, 1589.
(14) King, S. A.; Schwartz, J. *Inorg. Chem.* **1991**, *30*, 3771.
(15) Quignard, F.; Lecuyer, C.; Choplin, A.; Olivier, D.; Basset, J. M. *J. Mol. Catal.* **1992**, *74*, 353.
(16) Quignard, F.; Lecuyer, C.; Bougault, C.; Lefebvre, F.; Choplin, A.; Olivier, D.; Basset, J. M. *Inorg. Chem.* **1992**, *31*, 928.
(17) Corker, J.; Lefebvre, F.; Lecuyer, C.; Dufaud, V.; Quignard, F.; Choplin, A.; Evans, J.; Basset, J.-M. *Science* **1996**, *271*, 966.
(18) Lecuyer, C.; Quignard, F.; Choplin, A.; Olivier, D.; Basset, J. M. *Angew. Chem.* **1991**, *103*, 1692.

exchange reaction in H_2/D_2 or D_2/CH_4 mixtures,[19,20] and (3) low-temperature hydrogenolysis of alkanes.[18] More recently, it was shown that this highly electrophilic surface complex catalyzes the depolymerization of polyolefins via successive β-alkyl transfer−hydrogenolysis steps, the former being the reverse step of the Ziegler−Natta polymerization.[21] One key feature of this process is the transformation of polyolefins (e.g., polyethylene and polypropylene) back to low molecular weight alkanes.

The unexpected high reactivity of this tetracoordinated monohydrido zirconium species toward alkanes[22−25] (especially as compared to group 4 molecular equivalents)[26−32] led us to further investigate its (their) structure(s), its (their) mechanism(s) of formation, and its (their) reactivity(ies) through the use of advanced NMR spectroscopy techniques. We wish to report here that the synthesis of this zirconium monohydride leads also to the formation of a zirconium bis-hydride species. Their formation also results in the concomitant generation of surface silicon mono- and bis-hydride species, which allows to propose a mechanism for the surface reconstruction during the thermal treatment under hydrogen of $[(\equiv SiO)Zr(CH_2tBu)_3]$. The reactivity of these zirconium hydrides with N_2O and CO_2 is also reported and provides evidence for their difference in reactivity.

Results and Discussion

Spectroscopic Investigation of [Zr−H]. The reaction of $[(\equiv SiO)Zr(CH_2tBu)_3]$, obtained by reacting at 25 °C $[Zr(CH_2tBu)_4]$ on a silica partially dehydroxylated at 500 °C, with H_2 at 150 °C leads to the disappearance of more than 90% of the ν(C−H) and δ(C−H) according to in situ IR spectroscopy (Figure 1). New bands in the 2100−2300 and 1600−1650 cm^{-1} regions appear, which can be assigned to (Si−H) and (Zr−H), respectively, in agreement with the stretching frequencies of corresponding molecular complexes. Moreover, it has already been shown that upon treatment with D_2 at low temperatures (0−80 °C), the bands in the 1600−1650 cm^{-1} range disappeared, while those in the 2100−2300 cm^{-1} range remained unchanged, which further confirmed these assignments.[15] Samples prepared by impregnation were further analyzed by ESR and ^1H NMR spectroscopies. While the former technique points to the presence of small amounts of Zr^{III} species, ca. 5% (see Supporting Information), the latter brings additional information: the spectrum displays four signals at 0.8, 4.4, 10.1, and 12.1 ppm (Figure 2a). First, the signals at 4.4 ppm can be readily assigned to (Si−H) protons.[33] Second, the signal at 0.8 ppm can be assigned to residual alkyl fragments, which did not

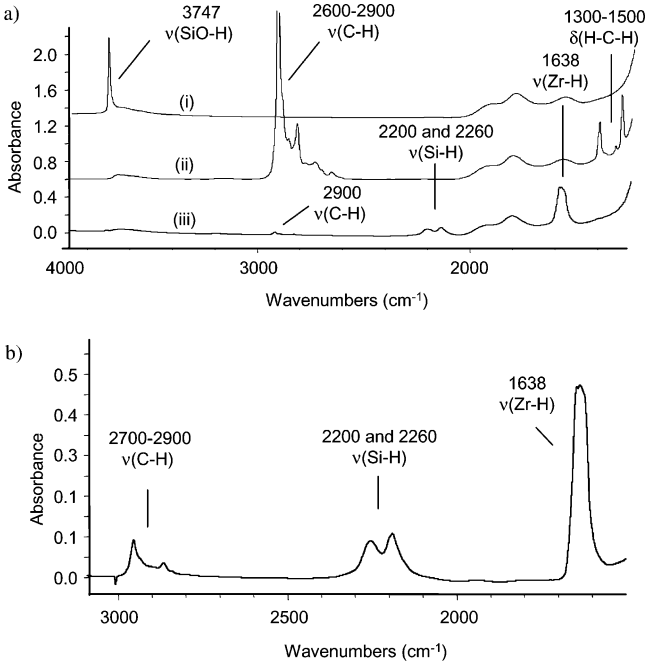

Figure 1. (a) Monitoring of the formation of [Zr−H] by IR spectroscopy: (i) $(SiO_{2-(500)})$, (ii) $[(\equiv SiO)Zr(CH_2tBu)_3]$, and (iii) after treatment under H_2 at 150 °C, [Zr−H]. (b) Enlargement of the 1500−3000 spectral region after subtraction of spectra iii−i of Figure 1a.

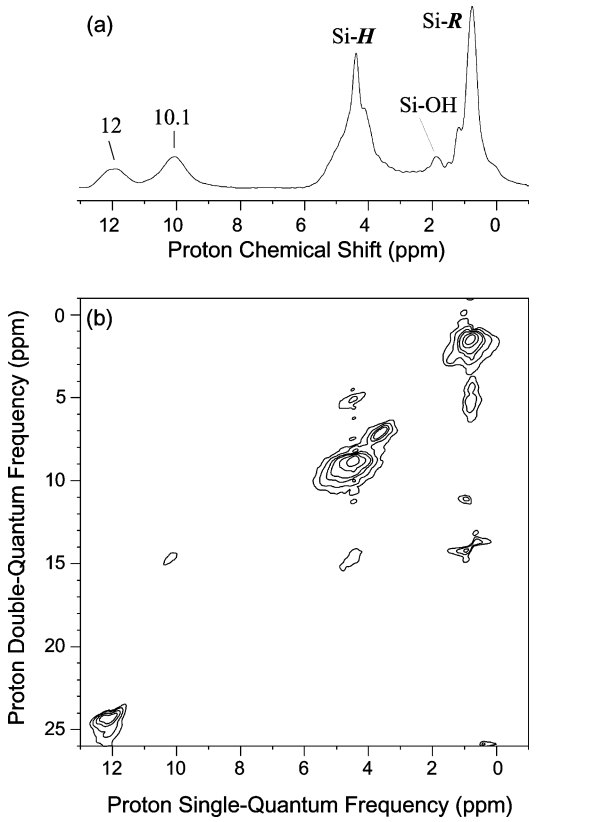

Figure 2. (a) ^1H MAS NMR spectrum of [Zr−H] species obtained as indicated in Scheme 1. (b) DQ rotor-synchronized 2D ^1H MAS spectrum of [Zr−H] species (see the Experimental Section for more details).

(19) Niccolai, G. P.; Basset, J.-M. *Appl. Catal. A* **1996**, *146*, 145.
(20) Casty, G. L.; Matturro, M. G.; Myers, G. R.; Reynolds, R. P.; Hall, R. B. *Organometallics* **2001**, *20*, 2246.
(21) Dufaud, V.; Basset, J.-M. *Angew. Chem., Int. Ed.* **1998**, *37*, 806.
(22) Mortensen, J. J.; Parrinello, M. *J. Phys. Chem. B* **2000**, *104*, 2901.
(23) Ustynyuk, L. Y.; Ustynyuk, Y. A.; Laikov, D. N.; Lunin, V. V. *Russ. Chem. Bull.* **2001**, *50*, 2050.
(24) Besedin, D. V.; Ustynyuk, L. Y.; Ustynyuk, Y. A.; Lunin, V. V. *Mendeleev Commun.* **2002**, 173.
(25) Copéret, C.; Grouiller, A.; Basset, J. M.; Chermette, H. *ChemPhysChem* **2003**, *4*, 609.
(26) Cummins, C. C.; Schaller, C. P.; Van Duyne, G. D.; Wolczanski, P. T.; Chan, A. W. E.; Hoffmann, R. *J. Am. Chem. Soc.* **1991**, *113*, 2985.
(27) Cummins, C. C.; Van Duyne, G. D.; Schaller, C. P.; Wolczanski, P. T. *Organometallics* **1991**, *10*, 164.
(28) Bennett, J. L.; Wolczanski, P. T. *J. Am. Chem. Soc.* **1994**, *116*, 2179.
(29) Schaller, C. P.; Bonanno, J. B.; Wolczanski, P. T. *J. Am. Chem. Soc.* **1994**, *116*, 4133.
(30) Wolczanski, P. T. *Polyhedron* **1995**, *14*, 3335.
(31) Schaller, C. P.; Cummins, C. C.; Wolczanski, P. T. *J. Am. Chem. Soc.* **1996**, *118*, 591.
(32) Bennett, J. L.; Wolczanski, P. T. *J. Am. Chem. Soc.* **1997**, *119*, 10696.
(33) Campbell-Ferguson, H. J.; Ebsworth, E. A. V.; MacDiarmid, A. G.; Yoshioka, T. *J. Phys. Chem.* **1967**, *71*, 723.

undergo hydrogenolysis, suggesting that they are attached to a silicon atom.[34] Finally, we note the presence of two downfield signals at 10.1 and 12.1 ppm, which can be assigned to two types of zirconium hydride surface species.[35] This assignment is further reinforced since these signals disappear upon reaction with N_2O and CO_2 according to both IR and NMR spectroscopies (vide infra). Moreover, these two signals display very different T_1 values: for example, the signal at 12.1 ppm is not very much affected by the relaxation delay (RD $\geq$ 2 s), while for one to obtain a constant intensity of the signal at 10.1 ppm requires a longer relaxation delay, typically 30 s. This is consistent with the presence of two kinds of protons with very different environments: one, which relaxes readily, probably because it is close to other dipoles (efficient relaxation pathway), and another one, which does not have similar efficient dipolar relaxation pathways and hence a long T_1, probably a more isolated proton. To further assign these various signals, 2D multiple-quantum (MQ) proton spectroscopy under magic angle spinning (MAS) [36−40] was applied. Double- and triple-quantum proton spectroscopies under fast MAS have been recently shown to be powerful techniques to probe structural information and dynamics inherent to proton−proton dipolar couplings. These techniques have been successfully applied to the characterization of hydrogen-bonding structures,[39,41] $\pi-\pi$ packing arrangements,[42,43] and defect sites in zeolites.[44]

Figure 2b shows the rotor-synchronized ^{1}H DQ MAS spectrum recorded for [Zr−H] at a MAS frequency of 14 kHz using one cycle (of duration one rotor period) of the BABA recoupling method[45,46] for the excitation and reconversion of the double quantum (DQ) coherences (see the Experimental Section for more details). In this experiment, the evolution of the DQ coherence created between a pair of dipolar-coupled protons is observed during the indirect detection time t_1. The DQ frequency in the ω_1 dimension corresponds to the sum of the two single-quantum frequencies of the two coupled protons and correlates in the ω_2 dimension with the two corresponding proton resonances. Therefore, the observation of a DQ peak implies a close proximity between the two protons involved in this correlation.

In the 2D spectrum of Figure 2b, a strong autocorrelation peak is observed for the proton resonance at 12.1 ppm (24.2 ppm in the ω_1 dimension), which unambiguously allows the assignment of this resonance to the (ZrH_2) group, [(≡SiO)$_2$-ZrH_2] (**1b**). The proton resonance at 10.1 ppm shows only a weak correlation with the (SiH) resonance (14.5 ppm in the ω_1 dimension), which very likely corresponds to the correlation between the monohydride [(≡SiO)$_3$Zr−H] (**1a**) and the [(≡SiO)$_2$SiH$_2$] protons (vide infra).

As expected, strong autocorrelation peaks are observed for the alkyl (1.6 ppm in the ω_1 dimension) and for the [(≡SiO)$_2$SiH$_2$] proton resonances (8.8 ppm in the ω_1 dimension). Interestingly, there is a common double-quantum frequency (at about 5 ppm) between the (Si−H) resonance and the alkyl one, which indicates that the residual alkyl fragments are relatively close to the silicon hydride species and possibly correspond to a [(≡SiO)$_2$Si(H)(R)] species, which are probably formed through the transfer of an alkyl fragment from the organozirconium species onto silica during the thermal treatment under H_2 (eq 1).

$$(Zr-CH_2R) + (\equiv Si-O-Si\equiv) \rightarrow (\equiv Si-O-Zr) + (\equiv Si-CH_2R) \quad (1)$$

An additional autocorrelation peak at 7.2 ppm in the ω_1 dimension of weak intensity is also observed, which likely corresponds to a partial oxidation/hydrolysis of the zirconium hydrides into [(≡SiO)$_2$Zr(OH)$_2$] during the preparation of the sample. While oxidation of residual zirconium alkyl derivatives into alkoxide during the preparation of the sample could also display a signal at 3.6 ppm (vide infra), we favor its assignment to a [(≡SiO)$_2$Zr(OH)$_2$] species because residual alkyls attached to a Zr are present in much less than 10% of the total Zr (<0.1 equiv of alkanes upon addition of water) and are not affected upon addition of N_2O (according to IR spectroscopy, vide infra). The presence of [(≡SiO)$_2$SiH$_2$], [(≡SiO)$_2$Si(H)R], and [(≡SiO)$_3$SiH] is further confirmed by ^{29}Si solid-state NMR spectroscopy by the presence of three broad signals centered at −40, −80, and −105 ppm, which are typical of [(≡SiO)$_2$SiX$_2$] (X = H and/or R),[47] [(≡SiO)$_3$SiX] (X = H and/or R; commonly called T_3 site),[48] and [(≡SiO)$_3$SiOE] (commonly called Q site for E = H or Si), respectively. Moreover, correlations between the Si−H protons centered at 4.4 ppm (see traces at 4.8 and 4.2 ppm in the Supporting Information) and the signals at −40 and −80 ppm in the ^{29}Si dimension in the 2D ^{1}H−^{29}Si HETCOR solid-state NMR spectrum corroborate these assignments.[49]

In conclusion, under H_2 at 150 °C the zirconium−carbon bonds of [(≡SiO)Zr(CH_2tBu)$_3$] undergo hydrogenolysis to generate very reactive hydride intermediates such as [(≡SiO)-ZrH_3] (**1c**), which further react with the silica surface. Because silica is amorphous, a well-defined surface complex like [(≡SiO)Zr(CH_2tBu)$_3$] is in fact surrounded by different local environments, that is, different types of siloxane bridges formed during the dehydroxylation step. First, the putative intermediate [(≡SiO)ZrH_3] (**1c**) generates [(≡SiO)$_2ZrH_2$] (**1b**) and [(≡SiO)$_3$SiH] (Scheme 1). In some cases (roughly 70−80%), adjacent siloxane bridges are close enough to the zirconium center so that the surface complex [(≡SiO)$_2ZrH_2$] (**1b**) reacts further to yield [(≡SiO)$_3$ZrH] (**1a**) and [(≡SiO)$_2$SiH$_2$]. Besides this main process, there are small amounts of Zr^{III} species and

(34) ^{13}C NMR, IR spectroscopies and elemental analysis show that <10 wt % of the initial carbon remains on the surface, and these alkyl residues do not react with H_2O, which is consistent with their assignment to (Si−R) species.
(35) Turculet, L.; Tilley, T. D. *Organometallics* **2004**, *23*, 1542.
(36) Geen, H.; Titman, J. J.; Gottwald, J.; Spiess, H. W. *Chem. Phys. Lett.* **1994**, *227*, 79.
(37) Geen, H.; Titman, J. J.; Gottwald, J.; Spiess, H. W. *J. Magn. Reson., Ser. A* **1995**, *114*, 264.
(38) Friedrich, U.; Schnell, I.; Demco, D. E.; Spiess, H. W. *Chem. Phys. Lett.* **1998**, *285*, 49.
(39) Schnell, I.; Brown, S. P.; Low, H. Y.; Ishida, H.; Spiess, H. W. *J. Am. Chem. Soc.* **1998**, *120*, 11784.
(40) Brown, S. P.; Spiess, H. W. *Chem. Rev.* **2001**, *101*, 4125.
(41) Brown, S. P.; Zhu, X. X.; Saalwaechter, K.; Spiess, H. W. *J. Am. Chem. Soc.* **2001**, *123*, 4275.
(42) Brown, S. P.; Schnell, I.; Brand, J. D.; Muellen, K.; Spiess, H. W. *J. Am. Chem. Soc.* **1999**, *121*, 6712.
(43) Brown, S. P.; Schaller, T.; Seelbach, U. P.; Koziol, F.; Ochsenfeld, C.; Klarner, F.-G.; Spiess, H. W. *Angew. Chem., Int. Ed.* **2001**, *40*, 717.
(44) Shantz, D. F.; Schmedt auf der Guenne, J.; Koller, H.; Lobo, R. F. *J. Am. Chem. Soc.* **2000**, *122*, 6659.
(45) Sommer, W.; Gottwald, J.; Demco, D. E.; Spiess, H. W. *J. Magn. Reson., Ser. A* **1995**, *113*, 131.
(46) Graf, R.; Demco, D. E.; Gottwald, J.; Hafner, S.; Spiess, H. W. *J. Chem. Phys.* **1997**, *106*, 885.
(47) Seyferth, D.; Prud'homme, C.; Wiseman, G. H. *Inorg. Chem.* **1983**, *22*, 2163.
(48) Marsmann, H. In *NMR, Basic Principles and Progress*; Kintzinger, J. P., Marsmann, H., Eds.; Springer-Verlag: New York, 1981; Vol. 17, p 65.
(49) However, recording good ^{29}Si solid-state NMR spectra has been of some difficulty for such type of material because the concentration is really low (10−50 mmol/g of sample), thus leading to a poor signal-to-noise ratio despite long experimental time (2 days and 6 days for the 1D and the 2D experiments, respectively).

Scheme 1. Reactivity of $[(\equiv SiO)Zr(CH_2tBu)_3]$ under H_2 at 150 °C

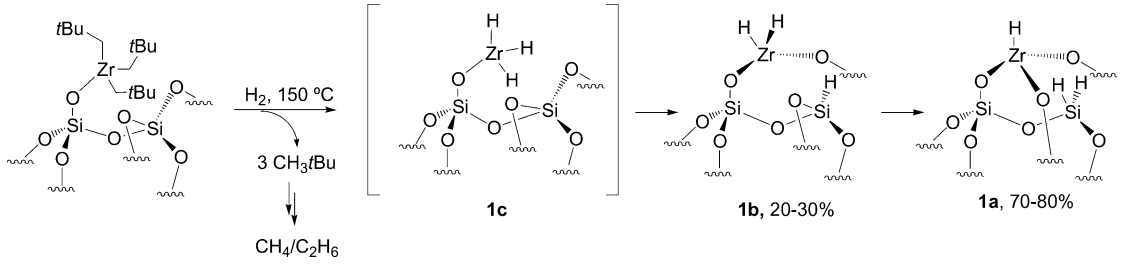

residual alkyl fragments, such as in $[(\equiv SiO)_2Si(H)(R)]$ fragments, which are probably formed through the transfer of alkyl zirconium species, such as $[(\equiv SiO)_{2-x}ZrH(R)_x]$ (eq 1).

Reactivity of [Zr−H] with H_2O. Hydrolysis has been used to characterize the hydride species through the measurement of hydrogen evolution, which was associated with the exclusive reaction of the metal hydrides with H_2O. Nevertheless, we have observed more recently that 1−2 equiv of H_2/Zr evolved during hydrolysis depending on the reaction conditions: the use of a small amount of water (2 equiv/Zr) and a short reaction time (∼15 min) reproducibly provided between 0.9 and 1.1 ± 0.2 equiv of H_2/Zr, while the use of a large excess of water (1500−2000 equiv/Zr) and a longer reaction time (2−12 h) led to 1.8−2.0 equiv of H_2/Zr. According to IR and ^{1}H NMR spectroscopies (see Supporting Information), H_2O mainly reacts with zirconium hydrides when used in stoichiometric amounts (2 equiv), while it reacts with zirconium hydrides and partially with surface (SiH_x) when a large excess (1500−2000 equiv) is used. In the latter case, the NMR spectrum is of poor quality, probably because of the major modification of the surface species (broad signals). Additionally, IR spectroscopy shows that only some (SiH_x) has reacted with H_2O (those at 2200 cm^{-1}), probably the (SiH_2). Yet, the reactivity of the surface (Si−H) fragments with H_2O is noteworthy because alkylsilanes (R_3SiH and R_2SiH_2) are usually not very reactive toward H_2O under identical conditions. This speaks in favor of an assistance of the zirconium center in the hydrolysis of the adjacent silanes and thereby shows that the zirconium center is in close proximity to the (Si−H) fragments, as was already shown by ^{1}H DQ MAS NMR spectroscopy applied to zirconium hydrides. This further confirms that the (Si−H) fragments are formed during the formation of zirconium hydrides through its reaction with adjacent siloxane bridges and not through the reaction of hydrogen directly with some siloxane bridges present at the surface of silica. However, the reaction of H_2O with [Zr−H] is quite complex and does not provide a clear molecular understanding of these surface species; therefore, different molecular probes have been used to understand these species.

Reactivity of [Zr−H] with CO_2. Metal hydrides are known to react with CO_2 to give metal formates.[50−53] Upon addition of CO_2 (300 equiv) onto [Zr−H], the ν(Zr−H) bands disappear immediately to give new bands at 1590/1386 and 1544/1370 cm^{-1} (Figure 3), assigned to the antisymmetric/symmetric stretching modes of the two different formate surface complexes. Moreover, two other weak bands also appear: one at 2960 cm^{-1},

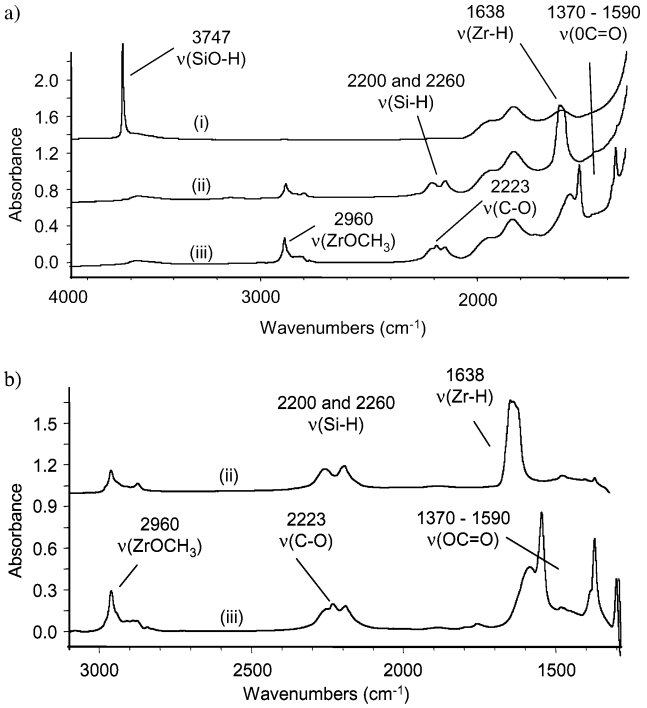

Figure 3. (a) Reaction of CO_2 with [Zr−H] monitored by IR spectroscopy: (i) ($SiO_{2-(500)}$), (ii) [Zr−H], and (iii) after reaction of [Zr−H] with CO_2 and evacuation of the excess CO_2 under vacuum. (b) Enlargement of the 1300−3000 spectral region of Figure 3a; spectra ii(b) and iii(b) correspond to (ii(a) − i(a)) and (iii(a) − ii(a)), respectively.

which is consistent with the formation of new C_{sp3}−H containing fragments, along with a very weak one at 2223 cm^{-1}. When using Zr−D in place of Zr−H, the band at 2960 cm^{-1} is shifted to 2180 cm^{-1}, in agreement with its assignment to a methoxy group (vide infra) formed upon reaction of the deuteride (hydride) ligand with CO_2 (see Supporting Information), while the band at 2223 cm^{-1} is not affected, which shows that it is most likely associated with the vibration of a C−O bond. When using $^{13}CO_2$, this latter band is shifted by 53 cm^{-1} to 2170 cm^{-1} in agreement with its assignment to a C−O bond. Free and coordinated CO_2 do not appear in this region,[54,55] while a CO bound to a Lewis center as a purely σ-donor ligand might.[11,56−58] However, this weak band (2170 cm^{-1}) is not shifted upon thermal treatment at 80 °C in the presence of ^{12}CO (no CO exchange), and it is only shifted to lower wavenumber by 18 cm^{-1} upon addition of pyridine (see Supporting Information). Therefore, its assignment is most consistent with a harmonic

(50) Cutler, A.; Raja, M.; Todaro, A. *Inorg. Chem.* **1987**, *26*, 2877.
(51) Mikhailova, O. A.; Minacheva, M. K.; Klemenkova, Z. S.; Shur, V. B. *Izv. Akad. Nauk, Ser. Khim.* **1996**, 2366.
(52) Schloerer, N. E.; Berger, S. *Organometallics* **2001**, *20*, 1703.
(53) Schloerer, N. E.; Cabrita, E. J.; Berger, S. *Angew. Chem., Int. Ed.* **2002**, *41*, 107.
(54) Yin, X.; Moss, J. R. *Coord. Chem. Rev.* **1999**, *181*, 27.
(55) Gibson, D. H. *Coord. Chem. Rev.* **1999**, *185−186*, 335.
(56) Davydov, A. A. *Infrared Spectroscopy of Adsorbed Species on the Surface of Transition Metal Oxides*; Wiley: Chichester, 1990.
(57) Ballinger, T. H.; Yates, J. T., Jr. *Langmuir* **1991**, *7*, 3041.
(58) Bolis, V.; Morterra, C.; Fubini, B.; Ugliengo, P.; Garrone, E. *Langmuir* **1993**, *9*, 1521.

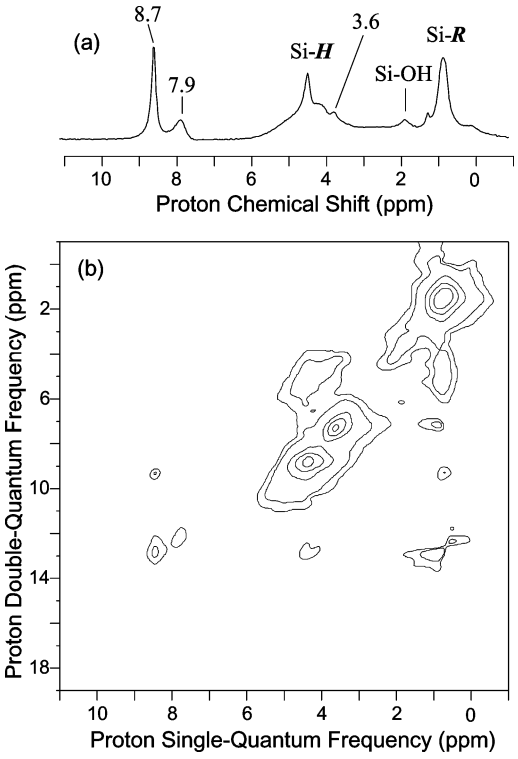

Figure 4. (a) ^{1}H MAS NMR spectra of [Zr−H] after reaction with CO_2 (as indicated in Scheme 2). (b) DQ rotor synchronized 2D ^{1}H MAS spectrum of [Zr−H] after reaction with CO_2 (see Experimental Section for more details).

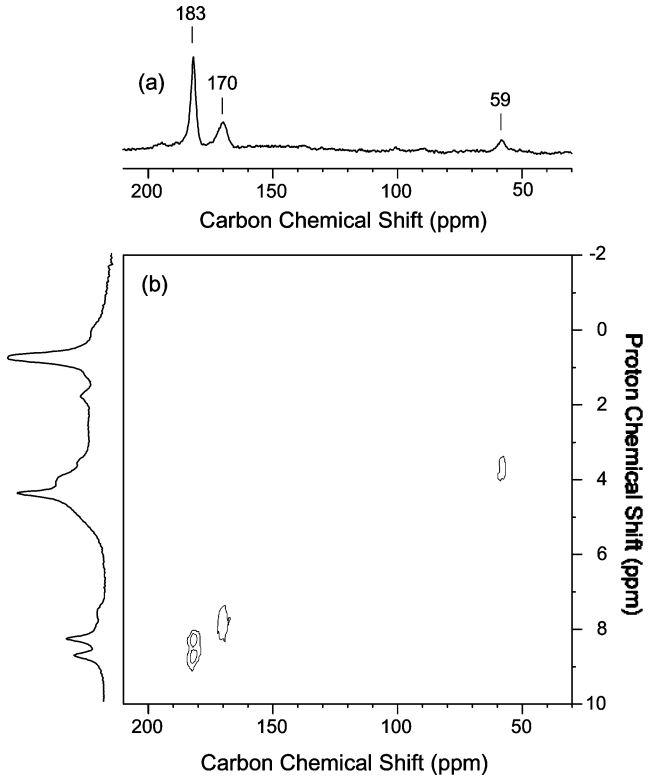

Figure 5. (a) ^{13}C CPMAS NMR spectrum of [Zr−H] after reaction with $^{13}CO_2$ (number of scans = 3618). (b) 2D carbon−proton heteronuclear dipolar correlation spectrum of [Zr−H] after reaction with $^{13}CO_2$ (see the Experimental Section for more details). The corresponding proton spectrum is shown on the left side of the 2D map.

of a C−O vibration in [ZrO−C(=O)H] (the fundamental vibration should appear in the 1100−1200 cm^{-1} region, but is masked by the silica framework vibrations).

According to ^{1}H solid-state NMR spectroscopy, the two signals, associated with the two types of hydrides, disappear upon addition of CO_2, while two new ones appear at 7.9 and 8.7 ppm in a 1/3 to 1/4 ratio (Figure 4). The chemical shifts of these new signals are consistent with the formation of formate zirconium complexes and can be assigned to the bis(formate) and monoformate species, respectively.[50−53] Besides, there is a shoulder peak next to the (SiH_x) signals at 3.6 ppm, which could be associated with the formation of downfield C_{sp3}−H protons, that of a methoxy fragment (vide infra), and which is consistent with what has been observed by IR spectroscopy. The DQ ^{1}H MAS NMR spectrum (Figure 4b) shows autocorrelation peaks for high field signals at 1.0 ppm (2.0 ppm in the ω_1 dimension, residual alkyl fragments), 3.6 ppm (7.2 ppm in the ω_1 dimension, $ZrOCH_3$), and 4.4 ppm (8.8 ppm in the ω_1 dimension, SiH_2). No autocorrelation peaks are found for either of the formate protons (they are expected to be very far apart for a bisformate complex). Residual alkyl fragments still show a correlation peak with the (Si−H) surface species, but also with the signal at 8.7 ppm assigned to the monoformate (at 9.5 ppm in the ω_1 dimension). This signal at 8.7 ppm (monoformate, **2a**) also shows a correlation with the (SiH_2) fragment (and vice versa) at 13.1 ppm in the ω_1 dimension. Note that the monohydride zirconium species [(≡SiO)$_3$ZrH] (**1a**) already showed a correlation peak with this (SiH_2) fragment. Moreover, the signals at 7.9 ppm (bisformate, **2b**) give rise to a signal at 12.3 ppm (in the ω_1 dimension), which shows that, upon insertion of CO_2, the proton is in proximity to (Si−H) fragments; the corresponding hydride (**1b**) did not show such type of correlation. To further characterize these species, a ^{13}C-labeled sample was prepared using ^{13}C-labeled CO_2. The ^{13}C NMR spectrum exhibits three major resolved peaks at 183, 170, and 59 ppm (Figure 5a). A two-dimensional ^{13}C−^{1}H HETCOR shows that correlation peaks are observed between proton resonances at 7.9 and 8.7 ppm in the ω_1 dimension and carbon resonances at 170 and 183 ppm in the ω_2 dimension, respectively (Figure 5b), confirming their assignments to two types of zirconium formate surface complexes (**2a** and **2b**). On this ^{13}C-labeled material, the carbon−proton scalar couplings can be directly estimated on the ^{1}H traces extracted in the ω_1 dimension of the 2D map (each formate proton appears as a doublet). Splittings of about 230 and 220 Hz were, respectively, measured for the carbon resonances at 170 and 183 ppm as may be expected for a formate ligand. The carbon peak at 59 ppm, which correlates with a proton resonance at 3.6 ppm, displays a J_{C-H} splitting of about 140 Hz, which is fully consistent with a heteroatom substituted sp^3 carbon, like a methoxy fragment. To further characterize these compounds, solid-state *J*-resolved spectroscopy was applied (Figure 6). The corresponding 2D spectrum shows that the carbon signal at 59 ppm is split into a quartet (J_{CH} = 128 ± 15 Hz) with a more or less 1:3:3:1 intensity distribution in the ω_1 dimension, which allows the straightforward identification of this resonance as a methoxy group. As expected at lower field, two carbon resonances (170 and 183 ppm) exhibit a doublet structure with J_{CH} coupling values of 252 and 243 Hz (±15 Hz), respectively. This is in relatively good agreement with the value obtained from the 2D HETCOR spectrum and direct detection.

The presence of two types of formate signals in IR, ^{1}H, and

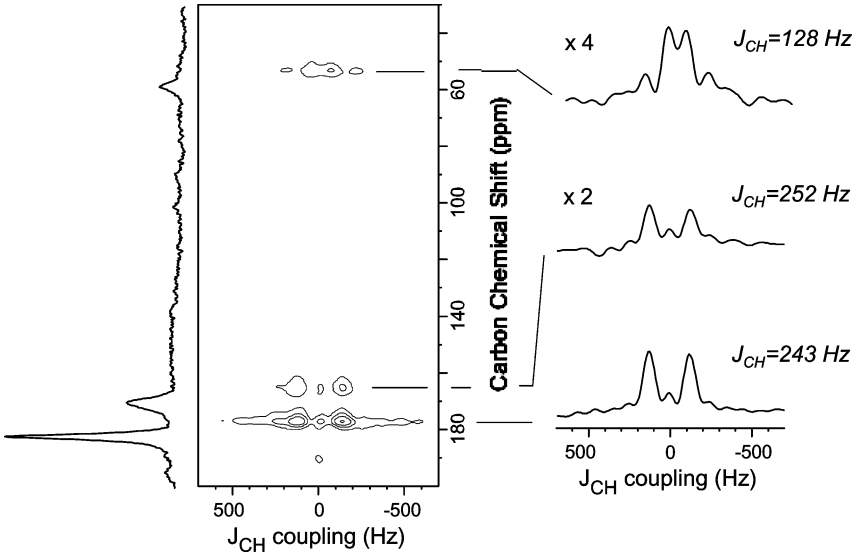

Figure 6. Carbon−proton solid-state *J*-resolved spectroscopy recorded on [Zr−H] after reaction with $^{13}CO_2$ (see the Experimental Section for more details).

Scheme 2. Reactivity of Zirconium Hydride Supported on Silica with CO_2

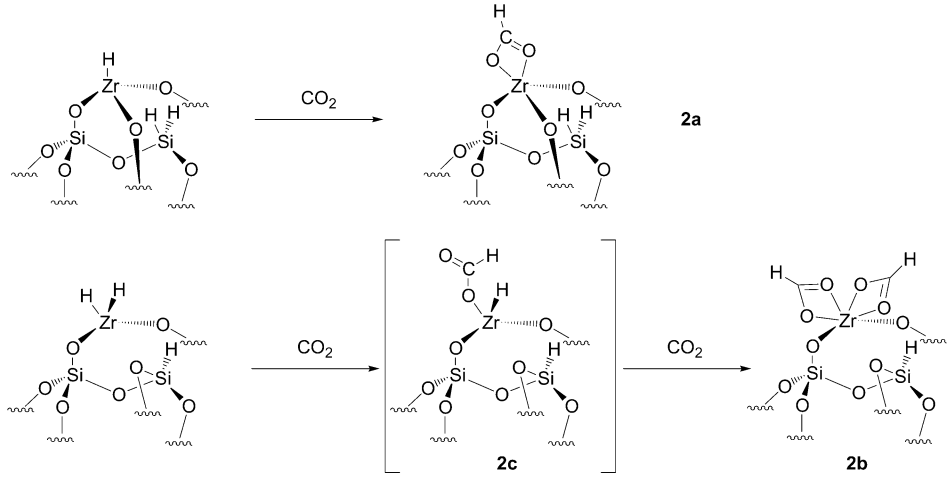

^{13}C NMR spectra can readily be explained by the reaction of CO_2 with the two different hydrides, leading to the formation of a mono(formate)tris(siloxy)zirconium complex (**2a**) and a bis(formate)bis(siloxy)zirconium complex (**2b**) (Scheme 2). In the case of the methoxy ligand, we propose that it arises from successive reactions of CO_2 with three hydrides via either the involvement of two sites (in average 6 Å apart) or the presence of small amount of a trishydride complex (not observed in ^1H NMR).[59]

Reactivity of [Zr−H] with N_2O. Metal hydrides can react cleanly with N_2O to give metal hydroxides,[60] and it constitutes a good probe reaction. Upon adding N_2O (300 equiv) to the silica-supported zirconium hydrides [Zr−H], most of the ν(Zr−H) band disappears immediately, and a new band appears at 3785 cm^{-1}, which is consistent with the formation of (Zr−OH) (Figure 7).[60−62] Moreover, a small amount of H_2 evolves (0.1−0.2 equiv/Zr) during this process, which could arise from the reductive elimination of H_2 from (ZrH_2), thus generating a Zr^{II} species, which is likely to be oxidized under these conditions.[63−65] Note that the (SiH_x) and alkyl surface species are not affected during this reaction. There is also the appearance of another band at 2145 cm^{-1} of variable and low intensity (depending on the reaction conditions: P_{N_2O}, temperature...). When using a fully deuterated sample (Zr−D/Si−D), the band at 3785 cm^{-1} (ZrO−H) is shifted to 2787 cm^{-1} as expected for the corresponding (ZrO−D) species, while the band at 2145 cm^{-1} is not shifted, which shows that it is probably associated with a N−N vibration arising from either N_2 or N_2O coordinated to a Zr center (see Supporting Information for details). ^1H MAS solid-state NMR spectroscopy also shows the disappearance of the two peaks at 10.1 and 12.1 ppm (Figure 8a), assigned to the two types of

(59) CO_2 reacts with [(≡$SiO)_2ZrH_2$] to yield the intermediate [(≡$SiO)_2$Zr(H)(−OC(δO)H)] (**2c**), which can react with another molecule of CO_2 to yield the bis(formate) complex [(≡$SiO)_2$Zr(−OC(=O)$H)_2$] (**2b**) or evolve into a 1,3-dioxa-2-zirconacyclobutane, [(≡$SiO)_2$Zr(η^2-OC(H_2)O] (not observed), which can decompose into "[(≡$SiO)_2$Zr=O]" (not identified) and formaldehyde as observed for similar molecular complexes (see refs 52 and 53). Formaldehyde can then react with an adjacent hydride to generate the methoxy zirconium surface complex.

(60) Vaughan, G. A.; Rupert, P. B.; Hillhouse, G. L. *J. Am. Chem. Soc.* **1987**, *109*, 5538.

(61) Dang, Z.; Anderson, B. G.; Amenomiya, Y.; Morrow, B. A. *J. Phys. Chem.* **1995**, *99*, 14437.

(62) Kytoekivi, A.; Lakomaa, E.-L.; Root, A.; Oesterholm, H.; Jacobs, J.-P.; Brongersma, H. H. *Langmuir* **1997**, *13*, 2717.

(63) Smith, M. R., III; Matsunaga, P. T.; Andersen, R. A. *J. Am. Chem. Soc.* **1993**, *115*, 7049.

(64) Howard, W. A.; Waters, M.; Parkin, G. *J. Am. Chem. Soc.* **1993**, *115*, 4917.

(65) Howard, W. A.; Parkin, G. *J. Am. Chem. Soc.* **1994**, *116*, 606.

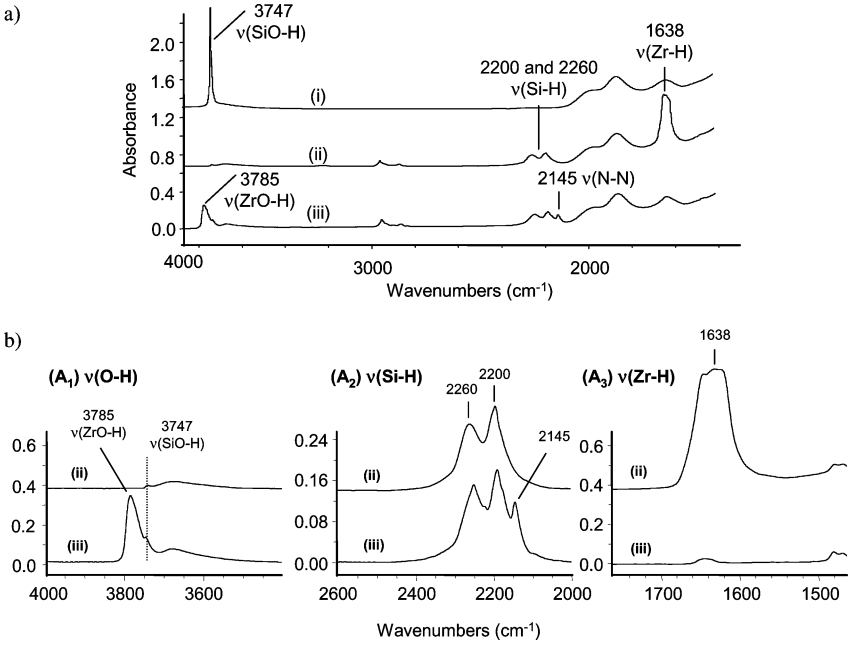

Figure 7. (a) Reaction of N_2O with [Zr−H] monitored by IR spectroscopy: (i) $SiO_{2-(500)}$, (ii) [Zr−H], (iii) after reaction of [Zr−H] with N_2O and evacuation of the excess N_2O under vacuum. (b) A_1, A_2, and A_3: Enlargement of the 3500−4000, 2100−2600, and 1500−1800 spectral regions of Figure 7a; for A_2 and A_3, spectra ii(b) and iii(b) correspond to (ii(a) − i(a)) and (iii(a) − ii(a)), respectively.

Scheme 3. Reactivity of Zirconium Hydride Supported on Silica with N_2O

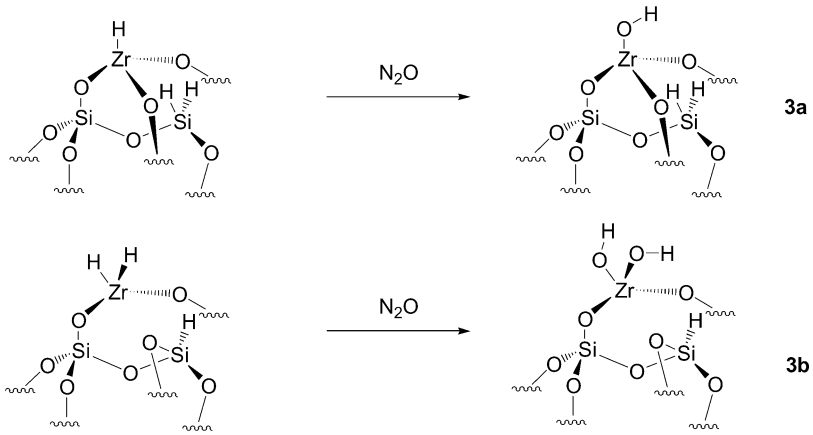

hydrides, and the concomitant appearance of two new signals at 3.6 and 4.1 ppm, whose chemical shifts are consistent with the formation of zirconium hydroxides.[60,66] The (Si−H) fragments are unaffected by this reaction as observed by IR spectroscopy (same vibration frequency and same intensity). Using double-quantum 2D ^{1}H NMR, we could assign the signal at 4.1 ppm to [(≡SiO)$_3$Zr(OH)], **3a** (due to the absence of such an autocorrelation peak), and that at 3.6 ppm to [(≡SiO)$_2$Zr-(OH)$_2$], **3b** (due to the observation of a clear autocorrelation peak at 7.2 ppm in the ω_1 dimension) (Figure 8b). Here also, a weak interaction between the residual alkyl and the (Si−H) fragments can be observed as in the case of zirconium hydrides (**1**). This material is stable up to 80−100 °C (see IR spectra in Supporting Information), and above this temperature the intensity of the [Zr(OH)] band (3785 cm^{-1}) starts to decrease to the advantage of that of the (Si−OH) bands (3747 cm^{-1}).[67] The material has a specific surface area of 190 m^2/g, which is comparable with the starting silica (190−200 m^2/g), and the chemical titration with methylmagnesium chloride shows the presence of about 1.2 ± 0.2 OH/nm^2, that is, 40 mmol OH/g, which is a little lower than that found for silica (1.4 ± 0.2 OH/nm^2 or 46 mmol OH/g). The presence of a large concentration of hydroxyl group is noteworthy because it is typically low for zirconia due to its small specific surface area. The nature of these (Zr−OH) fragments has been further investigated: the ^{15}N solid-state NMR spectrum of the solid contacted with ^{15}N-labeled pyridine displays one signal at −112 ppm, which is typical for a Lewis acid−Lewis base interaction, while no Brønsted acid character has been found (see Supporting

(66) Hillhouse, G. L.; Bercaw, J. E. *J. Am. Chem. Soc.* **1984**, *106*, 5472.

(67) After a treatment at 500 °C for 12 h under vacuum, there is only 30% of (Zr−OH) left, and the major components are (Si−OH) on the surface. Note that during this process some (Si−H) fragments are consumed, probably via reaction with the water produced during the condensation process (dehydroxylation).

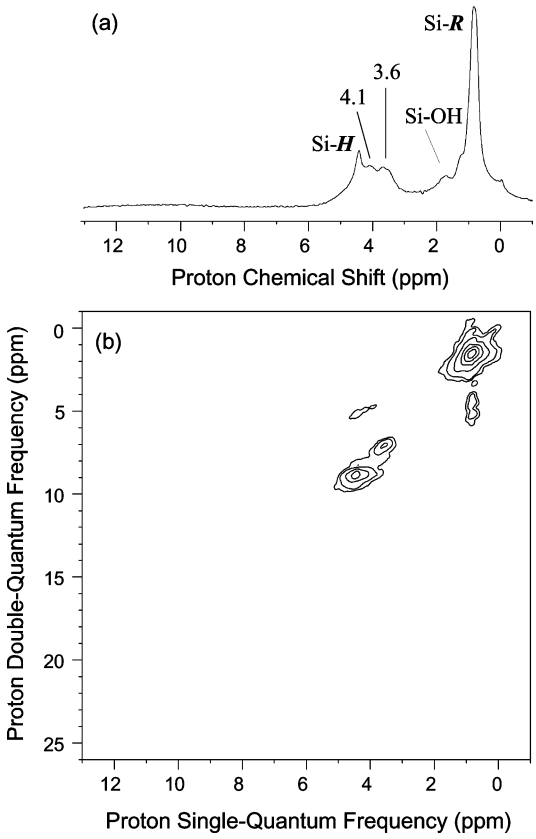

Figure 8. (a) ^{1}H MAS NMR spectrum of the [Zr−OH] species obtained as indicated in Scheme 3. (b) DQ rotor-synchronized 2D ^{1}H MAS spectrum of the [Zr−OH] species (see the Experimental Section for more details).

Information).[68] Furthermore, the ^{31}P solid-state NMR spectrum of the solid after treatment with triethylphosphine oxide (TEPO) shows two signals at 67.6 and 47.8 ppm,[69,70] corresponding to bound and free TEPO. The chemical shift difference is related to the acidic strength, and in this case it is in agreement with the strong Lewis acid character of Zr. Therefore, the data are consistent with a Zr center with a low coordination number, probably in a tetrahedral geometry like the precursors, which is also in agreement with the low Brønsted acid character of the hydroxyles in (ZrOH), **1**.[71] Note that molecular zirconium hydroxides are also fairly neutral and do not react with bases such as pyridine.[72]

Conclusion

We have shown that the combined use of reactivity studies and advanced solid-state NMR techniques is critical to ascertain the structure of surface complexes. DQ solid-state NMR is especially powerful because it can readily discriminate very similar structures such as (ZrX) and (ZrX_2) [X = −H, −OH, and −C(=O)H], but also provides information on the local environment of the metal centers (nonbonding interaction between the [Zr−H] and [Si−H]). This, in turn, also provides a better understanding of the influence of the local structure of silica on the structural identity of surface complexes: the reaction of a well-defined complex [(≡SiO)Zr(CH_2tBu)$_3$] with H_2 leads to the formation of a mixture of surface complexes [(≡SiO)$_2$ZrH_2] and [(≡SiO)$_3$Zr−H] along with (SiH_x) fragments via the opening of adjacent siloxane bridges. This reaction involves the reconstruction of the silica surface and translates quite well the heterogeneity of that surface as expected for an amorphous solid.

Experimental Details

General Procedure. All experiments were carried out under controlled atmosphere, using Schlenk and glovebox techniques for the organometallic synthesis. For the synthesis and treatments of the surface species, reactions were carried out using high-vacuum lines (1.34×10^{-3} kPa) and glovebox techniques. SiO_2 (Aerosil Degussa, 200 m^2 g^{-1}) was compacted with distilled water, calcined (400 °C under air), and partially dehydroxylated at 500 °C under vacuum (1.34×10^{-3} kPa) for 12 h (support referred to as $SiO_{2-(500)}$). [Zr(CH_2tBu)$_4$] was purchased from Aldrich. Pentane and diethyl ether were distilled on NaK alloy and benzophenone/Na, respectively, followed by degassing by freeze−pump−thaw cycles. Hydrogen was dried over freshly regenerated molecular sieves (3 Å) and deoxo traps; N_2O was purchased from Linde and used as received (purity of N_2O: 5.0); ^{15}N-pyridine was degassed by freeze−pump−thaw cycles; triethylphosphine oxide was evacuated under vacuum (1.34×10^{-3} kPa) at 25 °C for 1 h; CO_2 (Air Liquide) and $^{13}CO_2$ (Aldrich) were dried over molecular sieves. Infrared spectra were recorded on a Nicolet Magna 550 FT spectrometer equipped with a cell designed for in situ reactions under controlled atmosphere. Elemental analyses were performed at the Service Central d'Analyses of CNRS in Solaize. BET analyses were performed by the Laboratoire de Chimie Appliquée à l'Environnement of the CNRS/Université Lyon I. ^{1}H MAS, ^{13}C CP-MAS, ^{15}N CP-MAS, and ^{31}P HPDEC-MAS solid-state NMR spectra were recorded on a Bruker DSX-300 spectrometer. For specific studies (see below), ^{1}H MAS and ^{13}C CP-MAS solid-state NMR spectra were recorded on Bruker Avance-500 spectrometers with a conventional double resonance 4 mm CPMAS probe at the Laboratoire de Chimie at the Ecole Normale Supérieure de Lyon or in the Laboratoire de Chimie Organometallique de Surface at the Ecole Supérieure de Chimie Physique Electronique de Lyon. The samples were introduced under Ar in a zirconia rotor, which was then tightly closed. In all experiments, the rotation frequency was set to 10 kHz unless otherwise specified. Chemical shifts were given with respect to TMS, nitro-methane, and phosphoric acid (80%) as external references for ^{1}H−^{13}C, ^{15}N, and ^{31}P NMR, respectively.

Heteronuclear Correlation Spectroscopy. The two-dimensional heteronuclear correlation experiment was performed according to the following scheme: 90° proton pulse, t_1 evolution period, cross-polarization (CP) to carbon spins, detection of carbon magnetization. For the CP step, a ramped radio frequency (RF) field[73,74] centered at 60 kHz was applied on protons, while the carbon RF field was matched to obtain optimal signal. The contact time for CP was set to 1 ms. During acquisition, the proton decoupling field strength was set to 83 kHz (TPPM decoupling[75]). A total of 128 t_1 increments with 256 scans each were collected. The spinning frequency was 10 kHz, and the recycle delay was 2 s (total acquisition time of 5 h and 40 min). Quadrature detection in ω_1 was achieved using the TPPI method.[76] For ^{29}Si experiments, the spinning frequency was 4 kHz, the contact time for CP was set to 2 ms, the recycle delay was 1 s, and a total of 16 t_1 increments with 30 000 scans each were collected (total acquisition time: 6 days).

(68) Zhang, J.; Nicholas, J. B.; Haw, J. F. *Angew. Chem., Int. Ed.* **2000**, *39*, 3302.
(69) Osegovic, J. P.; Drago, R. S. *J. Catal.* **1999**, *182*, 1.
(70) Osegovic, J. P.; Drago, R. S. *J. Phys. Chem. B* **2000**, *104*, 147.
(71) Jolivet, J.-P. *Metal Oxide Chemistry and Synthesis. From Solution to Solid State*; Wiley: Chichester, 2000.
(72) Howard, W. A.; Trnka, T. M.; Waters, M.; Parkin, G. *J. Organomet. Chem.* **1997**, *528*, 95.
(73) Hediger, S.; Meier, B. H.; Kurur, N. D.; Bodenhausen, G.; Ernst, R. R. *Chem. Phys. Lett.* **1994**, *223*, 283.
(74) Metz, G.; Wu, X.; Smith, S. O. *J. Magn. Reson., Ser. A* **1994**, *110*, 219.
(75) Bennett, A. E.; Rienstra, C. M.; Auger, M.; Lakshmi, K. V.; Griffin, R. G. *J. Chem. Phys.* **1995**, *103*, 6951.
(76) Marion, D.; Wuethrich, K. *Biochem. Biophys. Res. Commun.* **1983**, *113*, 967.

***J*-Resolved Spectroscopy.** The two-dimensional *J*-resolved experiment was performed as previously described.[4] After cross-polarization from protons, carbon magnetization evolves during t_1 under proton homonuclear decoupling. Simultaneous 180° carbon and proton pulses are applied in the middle of t_1 to refocus the carbon chemical shift evolution while retaining the modulation by the heteronuclear J_{CH} scalar couplings. A Z-filter is finally applied to allow phase-sensitive detection in ω_1. Proton homonuclear decoupling was performed by using the frequency-switched Lee−Goldburg (FSLG) decoupling sequence.[77,78] Quadrature detection in ω_1 was achieved using the TPPI method.[76] The rotor spinning frequency was 10 204 kHz to synchronize the t_1 increment with the rotor period. The proton RF field strength was set to 83 kHz during t_1 (FSLG decoupling) and acquisition (TPPM decoupling).[75] The lengths of carbon and proton 180° pulses were 6.2 and 6 μs, respectively. An experimental scaling factor, measured as already described,[79] of 0.52 was found, which gave a corrected spectral width of 2452 Hz in the ω_1 dimension. The recycle delay was 2.5 s, and a total of 47 t_1 increments with 2048 scans each were collected.

Double-Quantum Spectroscopy. Two-dimensional double-quantum (DQ) experiments were performed according to the following general scheme: excitation of DQ coherences, t_1 evolution, reconversion into observable magnetization, Z-filter, and detection. The spectra were recorded in a rotor-synchronized fashion in t_1; that is, the t_1 increment was set equal to one rotor period. One cycle of the standard back-to-back (BABA) recoupling sequence[45,46] was used for the excitation and reconversion period. The standard BABA sequence, of duration one rotor period, takes the form $P_x-\tau-P_{-x}-P_y-\tau-P_{-y}$, where P_ϕ corresponds to a 90° proton pulse of phase ϕ, and τ equals $\tau_{R/2}$ minus the durations of two P_ϕ pulses (where τ_R is the rotor period). After the reconversion period, a delay of 200 μs was applied before the final 90° pulse (Z-filter). Quadrature detection in ω_1 was achieved using the States-TPPI method.[80] A spinning frequency of 14 kHz was used. The 90° proton pulse length was 3.1 μs, while a recycle delay of 2 s was used. A total of 96 t_1 increments of 7.142 μs with 128 scans each were recorded. The total experimental time for the DQ experiments was 6 h and 50 min.

Reaction of Silica with [Zr(CH$_2$*t*Bu)$_4$]: Formation of [(≡SiO)-Zr(CH$_2$*t*Bu)$_3$]. A mixture of [Zr(CH$_2$-*t*Bu)$_4$] (1.6 g, 4.26 mmol) in pentane (30 mL) and $SiO_{2-(500)}$ (8.4 g) was stirred at 25 °C for 2 h. After filtration, the solid was washed three times with pentane. The solvent was then removed, and the white solid was dried under dynamic-vacuum at 25 °C. ^{1}H MAS solid-state NMR (300 MHz, 25 °C): δ (ppm) 0.8 (s, C*H*$_2$, C*H*$_3$). ^{13}C CP-MAS solid-state NMR (300 MHz, 25 °C): δ (ppm) 34 (s, C(*C*H$_3$)$_3$), 95 (s, *C*H$_2$-*t*Bu). Infrared (cm^{-1}): 1300−1500 (s, δ(CH$_2$, CH$_3$)), 2600−2900 (s, ν(C−H)). Gas-phase analysis: 1 equiv/Zr of CH$_3$-*t*Bu evolved. Elemental analysis: %$_{wt}$ Zr 2.8, C 5.7.

Reaction of [(≡SiO)Zr(CH$_2$*t*Bu)$_3$] with H$_2$: Formation of the Silica-Supported Zirconium Hydride Species (1), [Zr−H]. In a 375 mL reactor, 3 g of [(≡SiO)Zr(CH$_2$*t*Bu)$_3$] (0.94 mmol of Zr) was treated with 76 kPa of H$_2$ (12 equiv/Zr). The temperature was increased to 150 °C (1 °C/min) and was maintained at this temperature for 6 h. The color of the solid turned rapidly from white to beige. A second treatment under H$_2$ was carried out to ensure a complete hydrogenolysis of the ligands and to yield [Zr−H]. ^{1}H MAS solid-state NMR (500 MHz, 25 °C): δ (ppm) 0.8 (s, Si−*R*), 1.8 (s, SiO−*H*), 4.4 (s, Si−*H* and Si*H*$_2$), 10.1 (s, Zr−*H*, **1a**), 12.1 (s, Zr*H*$_2$, **1b**). Infrared (cm^{-1}): 1638 (broad, ν(Zr−H) and ν(ZrH$_2$)), 2200, 2260 (m, ν(SiH) and ν(SiH$_2$)), 2600−2900 (w, ν(C−H)). Gas-phase analysis: a 3/1 mixture of CH$_4$ and C$_2$H$_6$ corresponding to 3 equiv/Zr of CH$_3$-*t*Bu was evolved. Elemental analysis: %$_{wt}$ Zr 2.8, C 0.53.

Reaction of [Zr−H] with a Stoichiometric Amount of H$_2$O. In a 25 mL reactor, 50 mg of [Zr−H] (0.016 mmol of Zr) was treated with 3.2 kPa of H$_2$O (0.032 mmol, 2 equiv/Zr). The color turned immediately from beige to white. After 10 min under H$_2$O atmosphere, the quantity of hydrogen (0.9−1.1 equiv/Zr) was measured by GC, and then the reactor was evacuated at 25 °C for 4 h (see Supporting Information for NMR spectra).

Reaction of [Zr−H] with a Large Excess of H$_2$O. In a 25 mL reactor, 50 mg of [Zr−H] (0.016 mmol of Zr) was treated with a large excess of H$_2$O (0.5 mL, 28 mmol, 1750 equiv/Zr). The color turned immediately from beige to white, and a gas evolution was observed. After 2 h under H$_2$O atmosphere, the quantity of hydrogen (1.8−2.0 equiv/Zr) was measured by GC, and then the reactor was evacuated at 25 °C for 4 h (see Supporting Information for IR and NMR spectra).

Reaction of [Zr−H] with CO$_2$: Formation of the Supported Zirconium Formate Species (2), [Zr−O(CO)H]. In a 375 mL reactor, 1 g of [Zr−H] (0.31 mmol of Zr) was treated with CO$_2$ (21.3 kPa, 3.1 mmol, 10 equiv/Zr). The color turned immediately from beige to white. After 3 h under CO$_2$ atmosphere, the reactor was evacuated at 25 °C for 2 h. ^{1}H MAS solid-state NMR (300 MHz, 25 °C): δ (ppm) 0.8 (s, Si−*R*), 1.8 (s, SiO−*H*), 3.6 (s, Zr−OC*H*$_3$), 4.4 (s, Si−*H* and Si*H*$_2$), 7.9 (s, [Zr(OC(=O)*H*)$_2$], **2b**), 8.5 (s, [Zr(OC(=O)−*H*)], **2a**). Infrared (cm^{-1}): 1386 and 1370 (s, ν_a(C=O)), 1590 and 1544 (s, ν_s(C=O)), 2200 and 2260 (w, ν(Si−H) and ν(SiH$_2$)), 2600−2900 (w, ν(C−H)).

Reaction of [Zr−H] with ^{13}CO$_2$: Formation of the Supported Zirconium Formate Species [Zr−O(^{13}CO)H]. See above. ^{1}H MAS solid-state NMR (300 MHz, 25 °C): δ (ppm) 0.8 (s, Si−*R*), 1.8 (s, SiO−*H*), 3.6 (bd, OC*H*$_3$), 4.4 (s, Si−*H* and Si*H*$_2$), 7.9 (bd, J_{C-H} = 226 Hz, [Zr(OC(=O)*H*)$_2$], **2b**), 8.7 (d, J_{C-H} = not measured directly, [Zr-(OC(=O)−*H*)], **2a**). ^{13}C CP-MAS solid-state NMR (300 MHz, 25 °C): δ (ppm) 59 (bs, [Zr(O*C*H$_3$)], **4**), 170 (bs, [Zr(O*C*(=O)H)$_2$], **2b**), 183 (bs, [Zr(O*C*(=O)H)], **2a**).

Reaction of [Zr−H] with N$_2$O: Formation of the Supported Zirconium Hydroxide Species (3), [Zr−OH]. In a 375 mL reactor, 1 g of [Zr−H] (0.31 mmol of Zr) was treated with N$_2$O (74 kPa, 11.2 mmol, 36 equiv/Zr) in the absence of light. The color turned immediately from beige to white. After 3 h at 25 °C, the gas phase was evacuated under dynamic-vacuum at 25 °C for 2 h. A second treatment under N$_2$O was carried out to ensure a complete consumption of the hydride. ^{1}H MAS solid-state NMR (500 MHz, 25 °C): δ (ppm) 0.8 (s, Si−*R*), 1.8 (s, SiO−*H*), 3.6 (s, Zr(O−*H*)$_2$, **3b**), 4.1 (s, ZrO−*H*, **3a**), 4.4 (s, Si−*H* and Si*H*$_2$). Infrared (cm^{-1}): 3785 (m, ν(ZrO−H)), 2900 (w, ν(C−H)), 2260 and 2200 (w, ν(Si−H) and ν(SiH$_2$)), 2145 (w). Gas-phase analysis: 0.15 equiv/Zr of H$_2$ evolved. Elemental analysis: %$_{wt}$ Zr: 2.8. BET surface area: 190 m^2 g^{-1}.

Determination of the Type of Surface Acidity for [Zr−OH] by Solid-State ^{15}N CP-MAS. Study of Chemisorption of Pyridine. Degassed ^{15}N-pyridine (60 μmol, 2 equiv/Zr) was introduced at 25 °C in a reactor containing 100 mg of [Zr−OH] (31 μmol of Zr). After 15 min, an excess of pyridine was eliminated under vacuum at 25 °C for 30 min, and the resulting solid was loaded into an NMR rotor in a glovebox. ^{15}N CP-MAS solid-state NMR (300 MHz, 25 °C): δ (ppm) −112.

Determination of Relative Surface Acidity Strengths for [Zr−OH] by Solid-State ^{31}P HPDEC-MAS. Study of Chemisorption of Triethylphosphine Oxide (TEPO). To a suspension of 250 mg of [Zr−OH] (77.5 μmol of Zr) in pentane (2 mL) was added 100 mg of TEPO (0.75 mmol, 9.6 equiv/Zr), and the mixture was stirred for 30 min. After evaporation of the solvent, the resulting solid was dried under dynamic-vacuum at 25 °C for 1 h and loaded into an NMR rotor in a glovebox. ^{31}P HPDEC-MAS solid-state NMR (300 MHz, 25 °C): δ (ppm) 47.8 (physisorbed TEPO), 67.6 (chemisorbed TEPO).

Determination of Surface Hydroxyl Density of [Zr−OH]. A 0.27 mol L^{-1} solution of [MeMgCl] in Et$_2$O (4 mL, 1.1 mmol) was

(77) Bielecki, A.; Kolbert, A. C.; Levitt, M. H. *Chem. Phys. Lett.* **1989**, *155*, 341.
(78) Levitt, M. H.; Kolbert, A. C.; Bielecki, A.; Ruben, D. J. *Solid State NMR* **1993**, *2*, 151.
(79) Lesage, A.; Duma, L.; Sakellariou, D.; Emsley, L. *J. Am. Chem. Soc.* **2001**, *123*, 5747.
(80) Marion, D.; Ikura, M.; Tschudin, R.; Bax, A. *J. Magn. Reson.* **1989**, *85*, 393.

introduced under argon at 25 °C in a reactor containing 200 mg of [Zr−OH] (62 μmol of Zr). The suspension was stirred for 2 h. The solvent and methane evolved were evaporated into a reactor of larger volume (2 L), and the resulting gaseous mixture was analyzed by gas chromatography. The amount of methane evolved was 78 μmol/0.2 g of solid, which corresponded to 390 μmol of hydroxyl groups/g of solid. For a specific area of 190 m^2 g^{-1}, the surface hydroxyl density corresponded to 1.2 $\pm$ 0.2 (−OH) nm^{-2}.

Acknowledgment. F.R. thanks the ministry of education, research & technology for a predoctoral fellowship. We are also grateful to Dr. M. Taoufik, Dr. D. Soulivong, and Prof. R. A. Andersen for helpful discussions. This work has been sponsored by BP Chemicals, CNRS, ENS Lyon, and ESCPE Lyon.

Supporting Information Available: Details of titration of Zr^{III} by EPR spectroscopy; additional IR and NMR spectra. This material is available free of charge via the Internet at http://pubs.acs.org.

JA038486H